SUPPLEMENTAL MATERIAL

Huggenberger et al., http://www.jem.org/cgi/content/full/jem.20100559/DC1

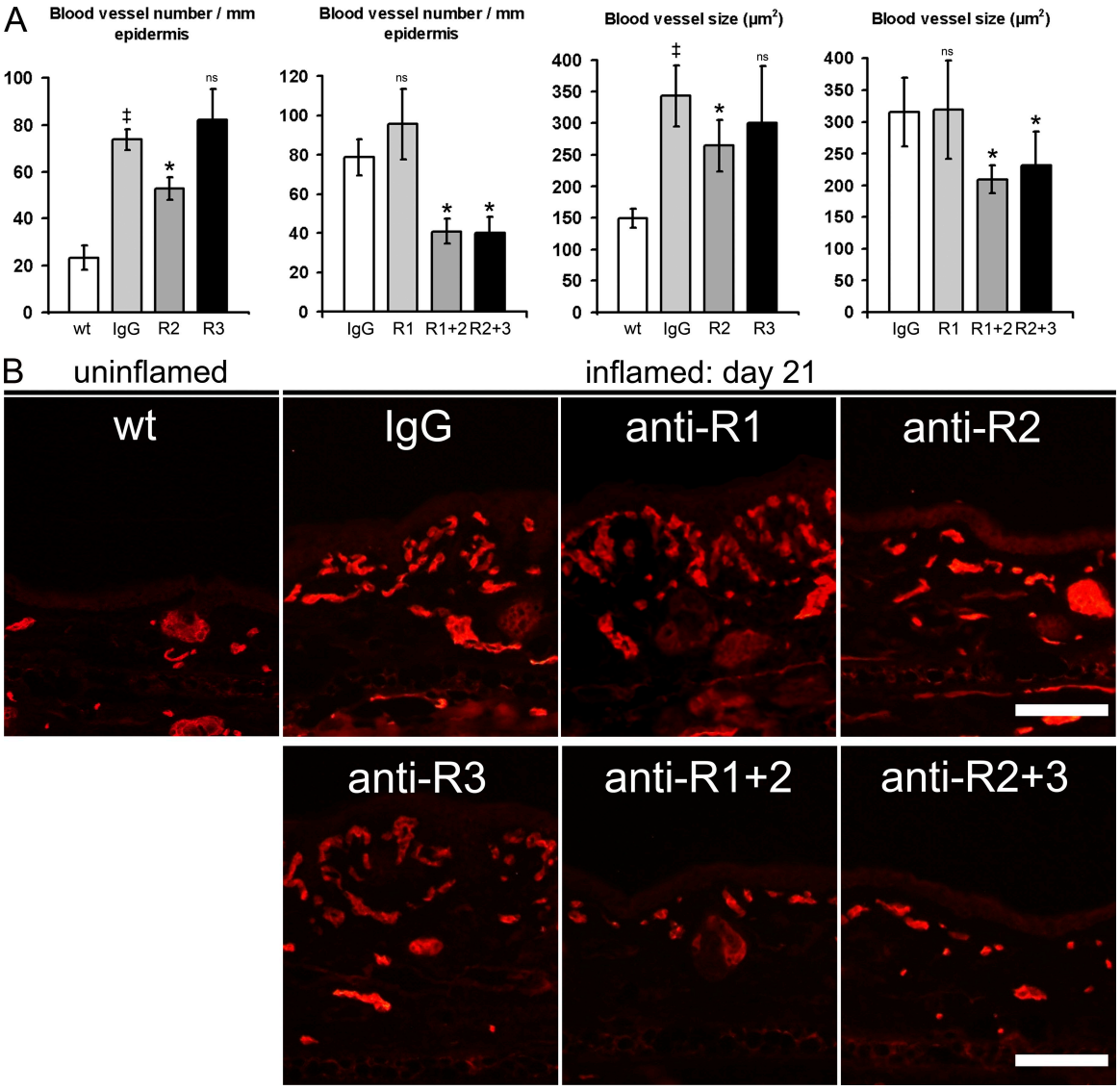

Figure S1. Inflammatory angiogenesis is inhibited by systemic blockade of VEGFR-2. (A) Immunofluorescence stainings of blood vessels (MECA32+) revealed a significantly increased number and size of blood vessels in control IgG-injected mice at day 21 after induction of inflammation, as compared with normal wild-type (wt) mice. The mean size and number of blood vessels after anti–VEGFR-1 (R1) or anti–VEGFR-3 (R3) mAb treatment was comparable to IgG-injected mice. Blood vessel number and size were significantly reduced after treatment with anti–VEGFR-2 (R2), anti–VEGFR-1+2 (R1+2), and anti–VEGFR-2+3 (R2+3) mAb. $n = 5$ mice per group. Two independent experiments were performed. Data represent mean ± SD. ‡, $P < 0.05$ versus wild type; *, $P < 0.05$ versus IgG. ns, not significant. (B) Representative images of MECA32-stained samples. Bars, 100 µm.

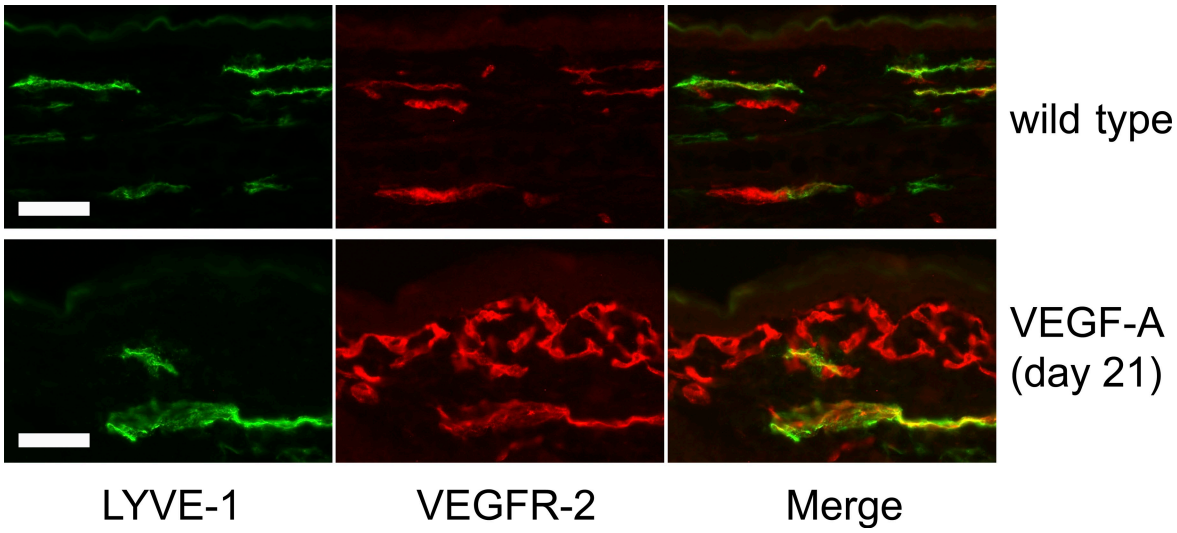

Figure S2. VEGFR-2 is expressed on lymphatic vessels in the ear skin of mice. LYVE-1$^+$ lymphatic vessels (green) express VEGFR-2 (red) in the ear skin of untreated wild-type mice and during chronic skin inflammation in the K14-VEGF-A Tg mice at 21 d after oxazolone challenge. The pictures shown are representative of findings in five mice each. Two independent experiments were performed. Bars, 50 µm.

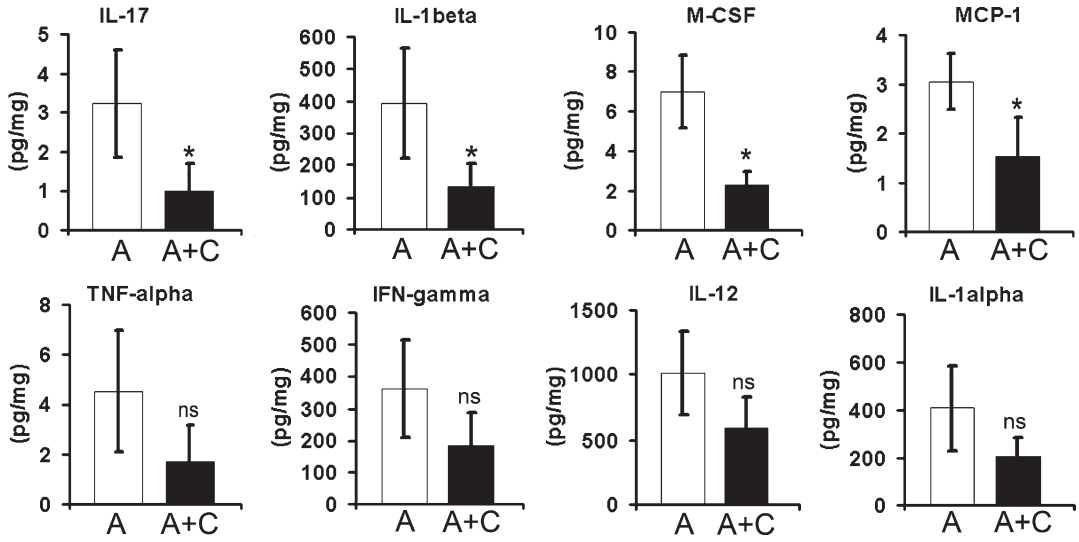

Figure S3. Tg overexpression of VEGF-C in the skin of K14–VEGF-A Tg mice results in reduced expression levels of inflammatory cytokines. A quantitative cytokine array was used to measure the protein levels of inflammation markers in K14-VEGF-A Tg mice (A) and K14-VEGF-A+C double Tg mice (A+C) at study day 28 after oxazolone challenge. Levels of IL-17, IL-1β, M-CSF, and MCP-1 were significantly lower in the skin of K14-VEGF-A/-C Tg mice than in K14-VEGF-A Tg mice. M-CSF, macrophage-specific CSF; MCP-1, monocyte chemotactic protein 1 (also termed CCL2). One experiment was performed with five mice per group. Data represent mean ± SD. *, $P < 0.05$. ns, not significant.

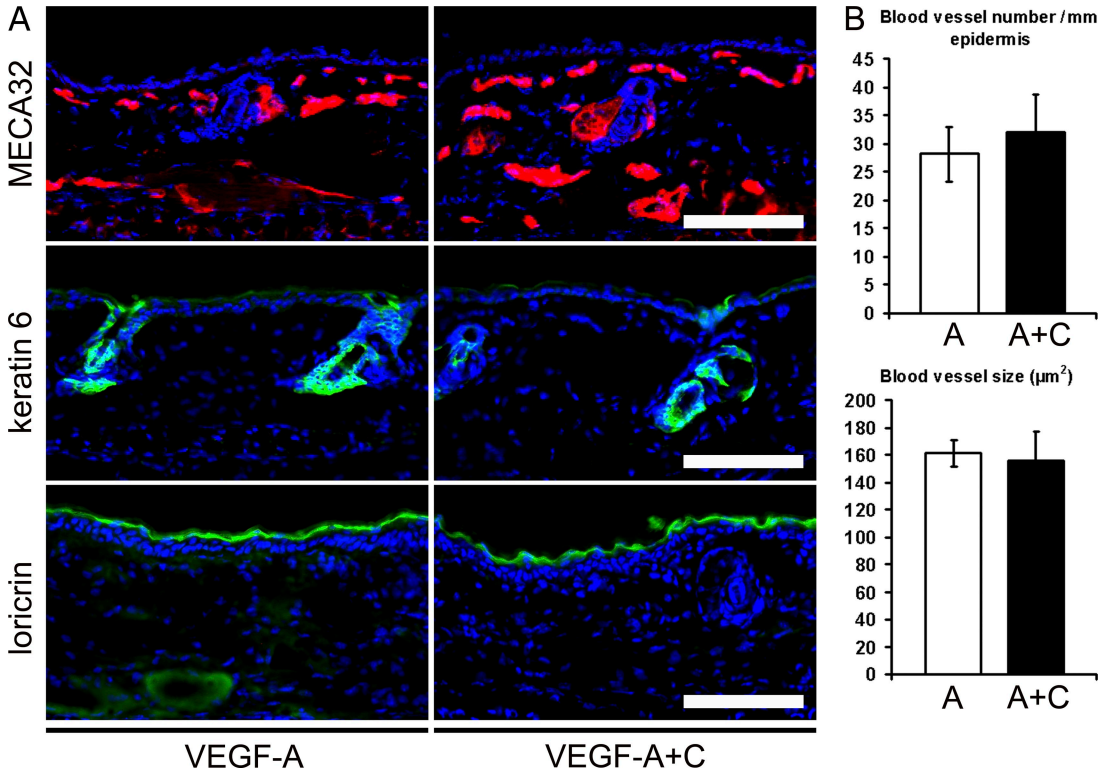

Figure S4. No baseline differences of vascularity and epidermal differentiation between unstimulated K14-VEGF-A and K14-VEGF-A+C Tg mice. (A and B) Shown are immunofluorescence and computer-assisted morphometric analyses for the blood vessel–specific marker MECA32, the hyperproliferation marker keratin 6, and the differentiation marker loricrin revealed a similar staining pattern (A) and a similar number and size of blood vessels (B) in K14-VEGF-A and in K14-VEGF-A+C Tg mice. Two independent experiments were performed with three mice per group. Data represent mean ± SD. Bars, 100 µm.

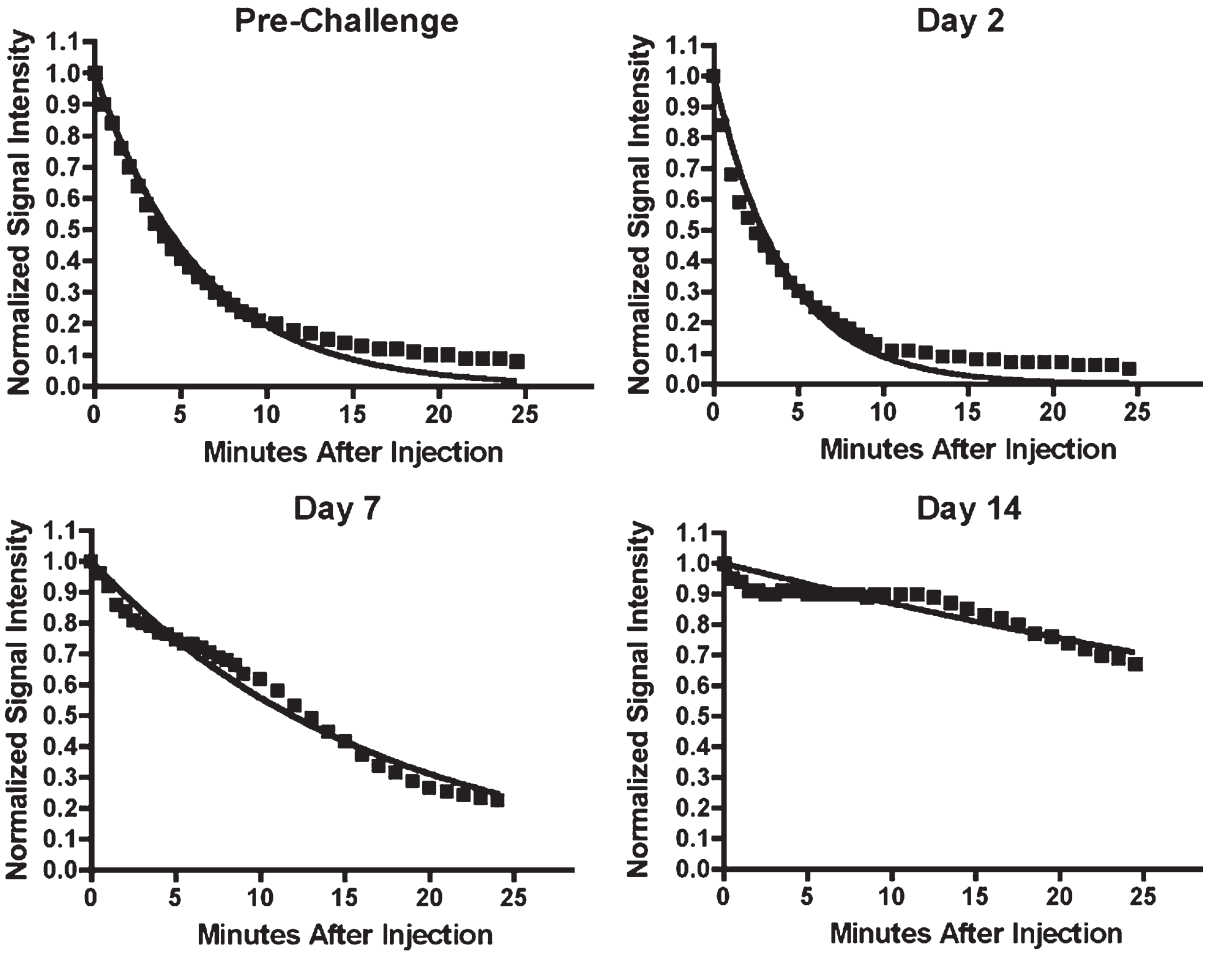

Figure S5. Representative curves of dye fluorescence intensity in the lymph node in the K14–VEGF-A mouse model. K14-VEGF-A Tg mice (n = 4) were sensitized and challenged using oxazolone. Indocyanine green–containing liposomes were injected intradermally into the ear skin and the lymphatic drainage from the superficial parotid lymph node was monitored in vivo using the IVIS system over a period of 25 min. In all conditions, the signal intensity reached its maximum in the superficial parotid lymph node within seconds after the injection of indocyanine green into the ear skin. We normalized the signal intensities measured over 25 min in the lymph node (see Fig. S6 for the exact localization of the lymph node) to the first/highest intensity measured. The curves were fitted with an exponential decay model. Pre-challenge: untreated/normal K14-VEGF-A Tg mice. Day 2, 7, 14: K14-VEGF-A Tg mice 2, 7, and 14 d after oxazolone challenge (n = 4). Two independent experiments were performed.

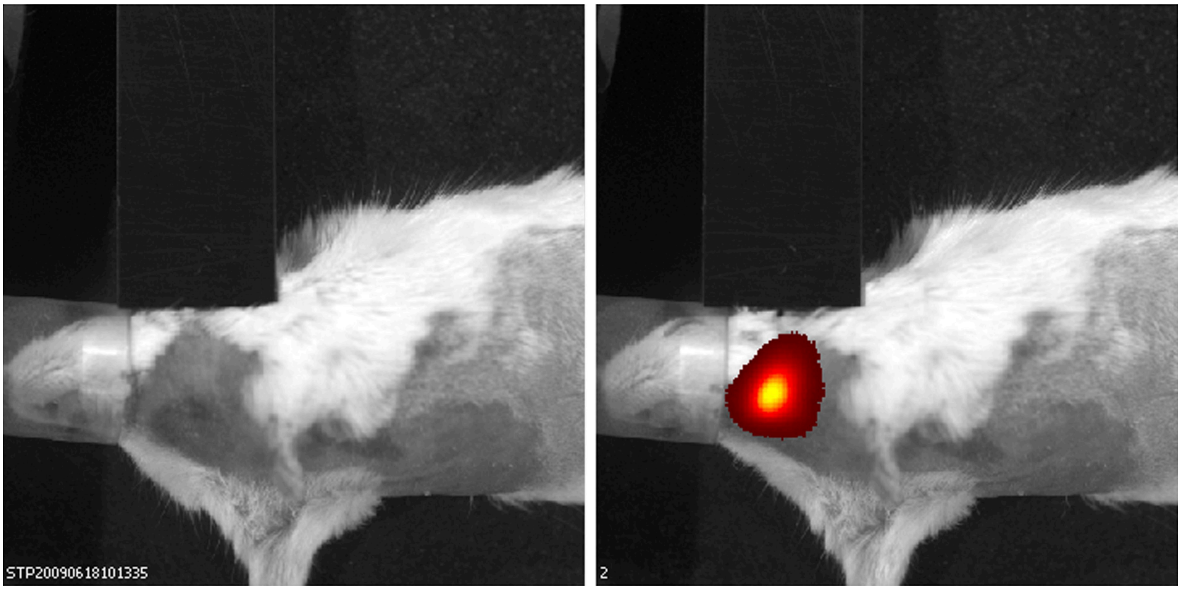

Figure S6. Localization of the superficial parotid lymph node. The image on the left shows a mouse positioned with its head toward the source of isoflurane. Before the injection of the dye, there is no signal in the shaved lymph node region. The image on the right shows that at 30 s after injection, a clear fluorescence signal is observed in the draining lymph node. The ear was covered after the injection.

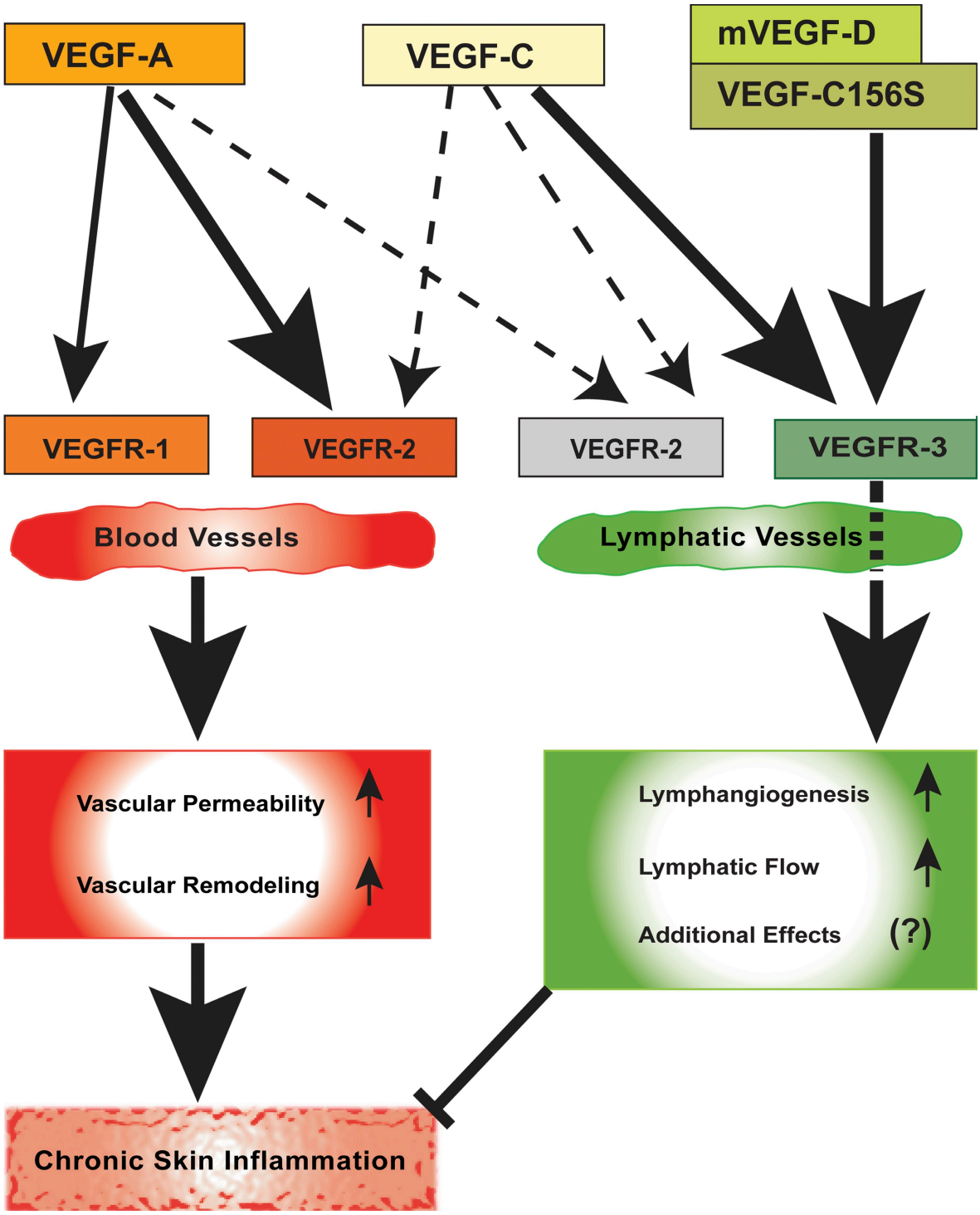

Figure S7. Role of angiogenesis and lymphangiogenesis in chronic skin inflammation. Blood vascular endothelial cells express VEGFR-1 and VEGFR-2, whereas lymphatic endothelial cells express VEGFR-2 and VEGFR-3. VEGF-A, which can bind both VEGFR-1 and VEGFR-2, can directly induce blood and lymphatic vascular remodeling. Chronic activation of the blood vasculature by VEGF-A leads to chronic skin inflammation. VEGF-C binds to VEGFR-3 and might also bind to VEGFR-2 (dashed arrows). In contrast, mouse VEGF-D (mVEGF-D) and VEGF-C156S are specific ligands for VEGFR-3. Stimulation of VEGFR-3 leads to lymphangiogenesis and can increase lymphatic flow. An expanded network of lymphatic vessels inhibits chronic skin inflammation. Additionally, collateral effects of lymphatic vessels, such as binding of chemokines, might contribute to the reduction of chronic inflammation.